

Decays $\tau \rightarrow (\eta, \eta')K^- \nu_\tau$ in the Extended Nambu–Jona-Lasinio Model¹

M. K. Volkov and A. A. Pivovarov

*Bogoliubov Laboratory of Theoretical Physics, Joint Institute for Nuclear Research,
Dubna, Moscow region, 141980 Russia*

e-mail: volkov@theor.jinr.ru

Received March 30, 2016

The decays $\tau \rightarrow (\eta, \eta')K^- \nu_\tau$ are described in the framework of the extended Nambu–Jona-Lasinio model. Both full and differential widths of these decays are calculated. The vector and scalar channels are considered. In the vector channel, the subprocesses with the intermediate $K^*(892)$ and $K^*(1410)$ mesons play the main role. In the scalar channel, the subprocesses with the intermediate $K_0^*(800)$ and $K_0^*(1430)$ mesons are taken into account. The scalar channel gives an insignificant contribution to the full width of the decay $\tau \rightarrow \eta K^- \nu_\tau$. The obtained results are in satisfactory agreement with the experimental data. The prediction for the width of the process $\tau \rightarrow \eta' K^- \nu_\tau$ is made.

DOI: 10.1134/S0021364016100106

1. INTRODUCTION

The τ -decays are a good laboratory for research of strong interactions of mesons at low energies. Since the perturbation theory of quantum chromodynamics is not applicable in this energy region (energy less than $m_\tau = 1.777$ GeV), one has to use different phenomenological models. These models are generally based on the vector dominance methods and on the chiral symmetry of strong interactions [1–10]. However, most of these models include a number of fitting parameters for a correct description of experimental data.

The Nambu–Jona-Lasinio (NJL) model [11–20] and its new version—the extended NJL model [20–24]—has a special place among them. These models allow one to avoid introduction of additional arbitrary parameters in the description of the hadron processes at low energies. The extended NJL model is especially useful for research of the τ -lepton decays. In the case of $U(3) \times U(3)$ chiral symmetry, this model allows describing meson nonets in both ground and first radially excited states. At the same time, due to the energy restrictions caused by the τ -lepton mass, intermediate mesons in these states play the main role in some τ -lepton decays. That is why, the use of the extended NJL model allowed a successful description of a series of τ -decays, specifically $\tau \rightarrow (\pi, \pi(1300))\nu_\tau$ [25], $\tau \rightarrow (\eta, \eta')\pi\nu_\tau$ [26], $\tau \rightarrow \pi\omega\nu_\tau$ [27], $\tau \rightarrow (\eta, \eta')2\pi$ [28], $\tau \rightarrow (\rho(770), \rho(1450))\nu_\tau$, $\tau \rightarrow (K^*(892), K^*(1410))\nu_\tau$ [29], $\tau \rightarrow K^-\pi^0\nu_\tau$ [30].

In the present work, these advantages of the extended NJL model are illustrated by the calculation of the width of the decay $\tau \rightarrow \eta K^- \nu_\tau$. Recently, this process has been actively investigated from both experimental [31, 32] and theoretical point of view. One of the most interesting theoretical works on this theme is [8]. In that paper the width of the decay $\tau \rightarrow \eta K^- \nu_\tau$ was calculated in the framework of Chiral Perturbation Theory extended by including resonances as active fields, and the prediction of the width of $\tau \rightarrow \eta' K^- \nu_\tau$ was made. In that work, it is asserted that the use of the Breit–Wigner parametrization does not give satisfactory results in the description of these processes. At the same time, two other methods based on the exponential resummation and dispersive representation provide good fits.

In our work, it is shown that in the framework of the extended NJL model the use of the Breit–Wigner relation in the standard form for description of the intermediate states leads to satisfactory results. This statement is confirmed by other calculations pointed above. We also make prediction of the width of the decay $\tau \rightarrow \eta' K^- \nu_\tau$, which agrees with the prediction in [8].

2. LAGRANGIAN OF THE EXTENDED NJL MODEL FOR THE MESONS $K^\pm, \eta, \eta', K^{*\pm}, K_0^{*\pm}$ AND THEIR FIRST RADIALLY EXCITED STATES

In the extended NJL model, the quark-meson interaction Lagrangian for the pseudoscalar K^\pm, η, η' ,

¹ The article is published in the original.

scalar $K_0^{*\pm}$, vector $K^{*\pm}$ mesons and their first radially excited states takes the form:

$$\begin{aligned} \Delta L_{\text{int}} = & \bar{q} \left[i\gamma^5 \sum_{j=\pm} \lambda_j (a_K K^j + b_K \hat{K}^j) \right. \\ & + \sum_{j=\pm} \lambda_j (a_{K_0^*} K_0^{*j} + b_{K_0^*} \hat{K}_0^{*j}) \\ & + \frac{1}{2} \gamma^\mu \sum_{j=\pm} \lambda_j (a_{K^*} K_\mu^{*j} + b_{K^*} \hat{K}_\mu^{*j}) \\ & \left. + i\gamma^5 \sum_{j=u,s} \lambda_j \sum_{\tilde{\eta}=\eta,\eta',\hat{\eta},\hat{\eta}'} A_{\tilde{\eta}}^j \tilde{\eta} \right] q, \end{aligned} \quad (1)$$

where q and \bar{q} are the u -, d -, and s -constituent quark fields with masses $m_u = m_d = 280$ MeV, $m_s = 420$ MeV [24, 33], η , η' , K^\pm , $K_0^{*\pm}$, and $K^{*\pm}$ are the pseudoscalar, scalar, and vector mesons; the excited states are marked with hat,

$$\begin{aligned} a_a &= \frac{1}{\sin(2\theta_a^0)} \\ &\times \left[g_a \sin(\theta_a + \theta_a^0) + g'_a f_a(\mathbf{k}^2) \sin(\theta_a - \theta_a^0) \right], \\ b_a &= \frac{-1}{\sin(2\theta_a^0)} \\ &\times \left[g_a \cos(\theta_a + \theta_a^0) + g'_a f_a(\mathbf{k}^2) \cos(\theta_a - \theta_a^0) \right], \\ A_{\tilde{\eta}}^j &= g_1^j b_{\tilde{\eta}1}^j + g_2^j f_j(\mathbf{k}^2) b_{\tilde{\eta}2}^j, \end{aligned} \quad (2)$$

$f(\mathbf{k}^2) = 1 + d\mathbf{k}^2$ is the form factor for description of the first radially excited states [21, 22], d is the slope parameter, θ_a and θ_a^0 are the mixing angles for the strange mesons in the ground and excited states,

$$\begin{aligned} d_{uu} &= -1.784 \text{ GeV}^{-2}, \quad d_{us} = -1.761 \text{ GeV}^{-2}, \\ d_{ss} &= -1.737 \text{ GeV}^{-2}, \\ \theta_K &= 58.11^\circ, \quad \theta_{K_0^*} = 74^\circ, \quad \theta_{K^*} = 84.74^\circ, \\ \theta_K^0 &= 55.52^\circ, \quad \theta_{K_0^*}^0 = 60^\circ, \quad \theta_{K^*}^0 = 59.56^\circ. \end{aligned} \quad (3)$$

The insertion of the pseudoscalar isoscalar fields requires consideration of the mixing of the four different states: η , $\eta'(958)$, $\eta(1295)$, $\eta(1475)$, which are marked as η , η' , $\hat{\eta}$, $\hat{\eta}'$. The last two ones are considered as the first radially excited states of the η and η' mesons; $b_{\hat{\eta}1}^j$ and $b_{\hat{\eta}2}^j$ are the mixing coefficients shown in table [24].

These coefficients were successfully applied for description of a series of processes with the η -mesons [24, 28, 34].

Mixing coefficients for the η -mesons

	η	$\hat{\eta}$	η'	$\hat{\eta}'$
$b_{\hat{\eta}1}^u$	0.71	0.62	-0.32	0.56
$b_{\hat{\eta}2}^u$	0.11	-0.87	-0.48	-0.54
$b_{\hat{\eta}1}^s$	0.62	0.19	0.56	-0.67
$b_{\hat{\eta}2}^s$	0.06	-0.66	0.30	0.82

The matrices

$$\begin{aligned} \lambda_+ &= \frac{\lambda_4 + i\lambda_5}{\sqrt{2}}, \quad \lambda_u = \frac{\sqrt{2}\lambda_0 + \lambda_8}{\sqrt{3}}, \\ \lambda_- &= \frac{\lambda_4 - i\lambda_5}{\sqrt{2}}, \quad \lambda_s = \frac{-\lambda_0 + \sqrt{2}\lambda_8}{\sqrt{3}}, \\ \lambda_0 &= \sqrt{\frac{2}{3}} \hat{1}, \end{aligned} \quad (4)$$

λ_4 , λ_5 , and λ_8 are the Gell-Mann matrices.

The coupling constants:

$$\begin{aligned} g_K &= \left(\frac{4}{Z_K} I_2(m_u, m_s) \right)^{-1/2} \approx 3.77, \\ g'_K &= \left(4I_2^{f_{us}^2}(m_u, m_s) \right)^{-1/2} \approx 4.69, \\ g_{K_0^*} &= \left(4I_2(m_u, m_s) \right)^{-1/2} \approx 2.78, \\ g'_{K_0^*} &= \left(4I_2^{f_{us}^2}(m_u, m_s) \right)^{-1/2} \approx 4.69, \\ g_{K^*} &= \left(\frac{2}{3} I_2(m_u, m_s) \right)^{-1/2} \approx 6.81, \\ g'_{K^*} &= \left(\frac{2}{3} I_2^{f_{us}^2}(m_u, m_s) \right)^{1/2} \approx 11.49, \\ g_1^u &= \left(\frac{4}{Z_\pi} I_2(m_u, m_u) \right)^{-1/2} \approx 3.02, \\ g_2^u &= \left(4I_2^{f_{uu}^2}(m_u, m_u) \right)^{-1/2} \approx 4.03, \\ g_1^s &= \left(\frac{4}{Z_s} I_2(m_s, m_s) \right)^{-1/2} \approx 4.41, \\ g_2^s &= \left(4I_2^{f_{ss}^2}(m_s, m_s) \right)^{-1/2} \approx 5.39, \end{aligned} \quad (5)$$

where

$$\begin{aligned} Z_\pi &= \left(1 - 6 \frac{m_u^2}{M_{a_1}^2} \right)^{-1} \approx 1.45, \\ Z_s &= \left(1 - 6 \frac{m_s^2}{M_{f_1}^2} \right)^{-1} \approx 2.09, \\ Z_K &= \left(1 - \frac{3(m_u + m_s)^2}{2 M_{K_1}^2} \right)^{-1} \approx 1.83, \end{aligned} \quad (6)$$

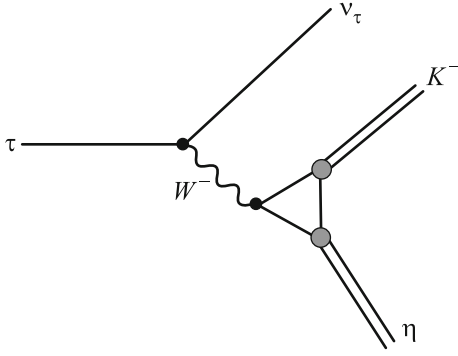


Fig. 1. Decay $\tau \rightarrow \eta K^- \nu_\tau$ with the intermediate W -boson (contact diagram).

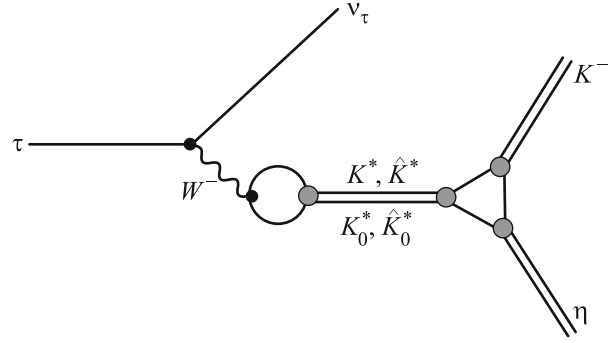


Fig. 2. Decay $\tau \rightarrow \eta K^- \nu_\tau$ with the intermediate vector $K^*(892)$, $K^*(1410)$ and scalar $K_0^*(800)$, $K_0^*(1430)$ mesons.

Z_π is the factor corresponding to the η – a_1 transitions, Z_K is the factor corresponding to the K – K_1 transitions, Z_s is the factor corresponding to the η – f_1 transitions, $M_{a_1} = 1230$ MeV, $M_{K_1} = 1272$ MeV, $M_{f_1} = 1426$ MeV [35] are the masses of the axial-vector a_1 , K_1 , and f_1 mesons, and the integral I_2 has the following form:

$$I_2^{f^n}(m_1, m_2) = -i \frac{N_c}{(2\pi)^4} \int \frac{f^n(\mathbf{k}^2)}{(m_1^2 - k^2)(m_2^2 - k^2)} \Theta(\Lambda_3^2 - \mathbf{k}^2) d^4k, \quad (7)$$

$\Lambda_3 = 1.03$ GeV is the cutoff parameter [14].

All these parameters were calculated earlier and are standard for the extended NJL model [22, 24].

3. AMPLITUDE OF THE DECAY $\tau \rightarrow \eta K^- \nu_\tau$ IN THE EXTENDED NJL MODEL

The diagrams of the process $\tau \rightarrow \eta K^- \nu_\tau$ are shown in Figs. 1 and 2.

3.1. Vector Channel

The amplitude of the process $\tau \rightarrow \eta K^- \nu_\tau$ for the vector channel takes the form:

$$T_V = -2iG_F |V_{us}| l^\mu \left\{ C_1 g_{\mu\nu} + \frac{C_2 C_3}{g_{K^*}} \times \frac{g_{\mu\nu} q^2 - q_\mu q_\nu - g_{\mu\nu} \frac{3}{2}(m_s - m_u)^2}{M_{K^*}^2 - q^2 - i\sqrt{q^2} \Gamma_{K^*}} + \frac{C_2' C_3'}{g_{K^*}} \times \frac{g_{\mu\nu} q^2 - q_\mu q_\nu - g_{\mu\nu} \frac{3}{2}(m_s - m_u)^2}{M_{\hat{K}^*}^2 - q^2 - i\sqrt{q^2} \Gamma_{\hat{K}^*}} \right\} (p_K - p_\eta)^\nu, \quad (8)$$

where $G_F = 1.16637 \times 10^{-11}$ MeV^{−2} is the Fermi constant, $V_{us} = 0.2252$ is the element of the Cabbibo–Kobayashi–Maskawa matrix, $l^\mu = \bar{\nu}_\tau \gamma^\mu \tau$ is the lepton current, $q = p_K + p_\eta$, $M_{K^*} = 896$ MeV, $M_{\hat{K}^*} =$

1414 MeV, $\Gamma_{K^*} = 46$ MeV, $\Gamma_{\hat{K}^*} = 232$ MeV are the masses and the full widths of the vector mesons [35].

The first term corresponds to the diagram with the intermediate W -boson, the second and the third terms correspond to the diagrams with the intermediate vector mesons $K^*(892)$ and $K^*(1410)$. The part

$$\frac{C_2(C_2')}{g_{K^*}} \left[g_{\mu\nu} q^2 - q_\mu q_\nu - g_{\mu\nu} \frac{3}{2}(m_s - m_u)^2 \right]$$

is obtained from the quark loop in the transition of the W -boson into the intermediate vector meson. The part $C_1(C_3, C_3')(p_K - p_\eta)^\nu$ comes from the quark triangle. The numerical coefficients are

$$\begin{aligned} C_1 &= I^{a_K A_\eta^u} + \sqrt{2} I^{a_K A_\eta^s}, \\ C_2 &= \frac{1}{\sin(2\theta_{K^*}^0)} [\sin(\theta_{K^*} + \theta_{K^*}^0) + R_V \sin(\theta_{K^*} - \theta_{K^*}^0)], \\ C_2' &= \frac{-1}{\sin(2\theta_{\hat{K}^*}^0)} [\cos(\theta_{K^*} + \theta_{K^*}^0) + R_V \cos(\theta_{K^*} - \theta_{K^*}^0)], \\ C_3 &= I^{a_K a_{K^*} A_\eta^u} + \sqrt{2} I^{a_K a_{K^*} A_\eta^s}, \\ C_3' &= I^{a_K b_{K^*} A_\eta^u} + \sqrt{2} I^{a_K b_{K^*} A_\eta^s}, \end{aligned} \quad (9)$$

where

$$R_V = \frac{I_2^{f_{us}}(m_u, m_s)}{\sqrt{I_2(m_u, m_s) I_2^{f_{us}}(m_u, m_s)}},$$

$$I^{abc} = -i \frac{N_c}{(2\pi)^4} \int \frac{a(\mathbf{k}^2) b(\mathbf{k}^2) c(\mathbf{k}^2)}{(m_s^2 - k^2)(m_u^2 - k^2)} \Theta(\Lambda_3^2 - \mathbf{k}^2) d^4k,$$

and where $a(\mathbf{k}^2)$, $b(\mathbf{k}^2)$, and $c(\mathbf{k}^2)$ are the coefficients from the Lagrangian defined in (2).

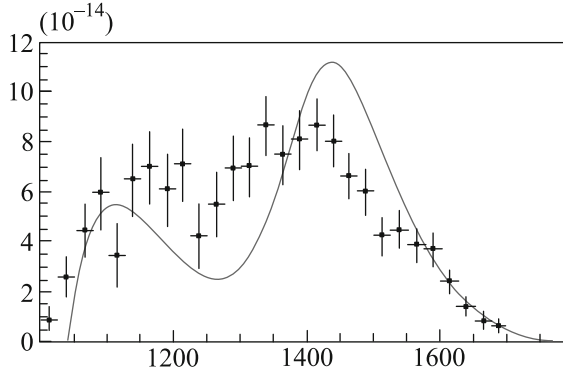


Fig. 3. Differential width of the decay $\tau \rightarrow \eta K^- \nu_\tau$.

3.2. Scalar Channel

The amplitude of the process $\tau \rightarrow \eta K^- \nu_\tau$ for the scalar channel takes the form

$$T_S = -4iG_F |V_{us}| l^\mu \times \left\{ \frac{C_4 C_5}{g_{K_0^*}} \frac{m_s - m_u}{M_{K_0^*}^2 - q^2 - i\sqrt{q^2} \Gamma_{K_0^*}} + \frac{C_4' C_5'}{g_{\tilde{K}_0^*}} \frac{m_s - m_u}{M_{\tilde{K}_0^*}^2 - q^2 - i\sqrt{q^2} \Gamma_{\tilde{K}_0^*}} \right\} q_\mu, \quad (10)$$

where $M_{K_0^*} = 682$ MeV, $M_{\tilde{K}_0^*} = 1425$ MeV, $\Gamma_{K_0^*} = 547$ MeV, and $\Gamma_{\tilde{K}_0^*} = 270$ MeV are the masses and full widths of the scalar mesons [35].

The part $\frac{C_4(C_4')}{g_{K_0^*}}(m_s - m_u)$ is obtained from the quark loop in the transition of the W -boson into the intermediate scalar meson. The part $C_5(C_5')q_\mu$ comes from the quark triangle. The numerical coefficients are

$$C_4 = \frac{1}{\sin(2\theta_{K_0^*}^0)} \times \left[\sin(\theta_{K_0^*} + \theta_{K_0^*}^0) + R_V \sin(\theta_{K_0^*} - \theta_{K_0^*}^0) \right],$$

$$C_4' = \frac{-1}{\sin(2\theta_{\tilde{K}_0^*}^0)} \times \left[\cos(\theta_{K_0^*} + \theta_{K_0^*}^0) + R_V \cos(\theta_{K_0^*} - \theta_{K_0^*}^0) \right], \quad (11)$$

$$C_5 = m_s I^{a_{K_0^*} a_{K_0^*}^s A_\eta^s} - \sqrt{2} m_u I^{a_{K_0^*} a_{K_0^*}^s A_\eta^s},$$

$$C_5' = m_s I^{a_{\tilde{K}_0^*} b_{\tilde{K}_0^*}^s A_\eta^s} - \sqrt{2} m_u I^{a_{\tilde{K}_0^*} b_{\tilde{K}_0^*}^s A_\eta^s}.$$

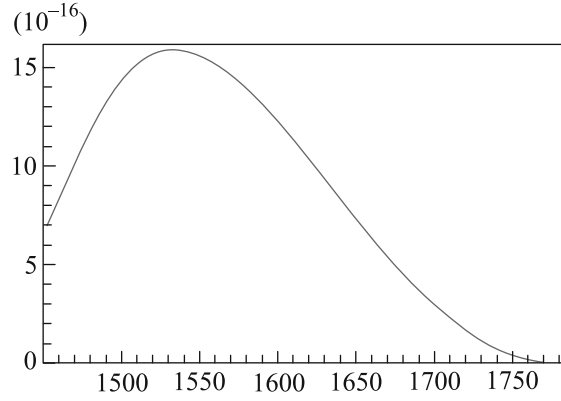


Fig. 4. Differential width of the decay $\tau \rightarrow \eta' K^- \nu_\tau$.

4. NUMERICAL ESTIMATES

The contribution of the diagrams with the vector channel to the branching of the process $\tau \rightarrow \eta K^- \nu_\tau$ is

$$Br(\tau \rightarrow \eta K^- \nu_\tau)_V = 1.46 \times 10^{-4}. \quad (12)$$

The contribution of the scalar channel is

$$Br(\tau \rightarrow \eta K^- \nu_\tau)_S = 0.28 \times 10^{-7}. \quad (13)$$

The calculated branching of the whole process is

$$Br(\tau \rightarrow \eta K^- \nu_\tau)_{\text{tot}} = 1.45 \times 10^{-4}. \quad (14)$$

The experimental values of this branching are

$$Br(\tau \rightarrow \eta K^- \nu_\tau)_{\text{exp}} = (1.58 \pm 0.14) \times 10^{-4} \quad [31],$$

$$Br(\tau \rightarrow \eta K^- \nu_\tau)_{\text{exp}} = (1.42 \pm 0.18) \times 10^{-4} \quad [32], \quad (15)$$

$$Br(\tau \rightarrow \eta K^- \nu_\tau)_{\text{exp}} = (1.52 \pm 0.08) \times 10^{-4} \quad [35].$$

In conclusion, let us note that we have not taken into account the dependence of the width of $K^*(892)$ on the momentum. If we assume that it grows linearly in $\sqrt{q^2}$, then in the considered energy region one can put $\Gamma_{K^*} \approx 70$ MeV. Then the whole branching is

$$Br(\tau \rightarrow \eta K^- \nu_\tau) = 1.54 \times 10^{-4}. \quad (16)$$

The comparison of the calculated and experimental differential widths is shown in Fig. 3. The solid line corresponds to our theoretical differential width. The points correspond to the experimental values [31].

The prediction for the branching of the process $\tau \rightarrow \eta' K^- \nu_\tau$ is obtained similarly. The contribution of the vector channel is

$$Br(\tau \rightarrow \eta' K^- \nu_\tau)_V = 1.69 \times 10^{-6}. \quad (17)$$

The contribution of the scalar channel is

$$Br(\tau \rightarrow \eta' K^- \nu_\tau)_S = 0.77 \times 10^{-7}. \quad (18)$$

The branching of the whole process is

$$Br(\tau \rightarrow \eta' K^- v_\tau)_{\text{tot}} = 1.25 \times 10^{-6}. \quad (19)$$

The experimental value is [35]

$$Br(\tau \rightarrow \eta' K^- v_\tau)_{\text{exp}} < 2.4 \times 10^{-6}. \quad (20)$$

The prediction of the differential width of the process $\tau \rightarrow \eta' K^- v_\tau$ is shown in Fig. 4.

5. CONCLUSIONS

The calculations carried out in the framework of the extended NJL model show that the main contribution to the width of the decay $\tau \rightarrow \eta K^- v_\tau$ is given by the vector channel. The subprocesses with the intermediate $K^*(892)$ and $K^*(1410)$ mesons play the principal role. The channel with the intermediate scalar mesons gives a negligible contribution. The obtained results are in satisfactory agreement with the experimental data. The prediction for the width of the process $\tau \rightarrow \eta' K^- v_\tau$ was made.

The right shift of the main peak of our theoretical differential width of the process $\tau \rightarrow \eta K^- v_\tau$ may be explained by a wrong choice of the mass of $K^*(1410)$, which is not measured precisely enough [36, 37]. The experimentally observed small bump of the differential width in the region of 1600 MeV may be explained by the existence of the second radially excited state $K^*(1680)$, which was not taken into account here.

We are grateful to A.B. Arbuzov and O.V. Teryaev for useful discussions. This work was supported by the Russian Foundation for Basic Research (project no. 14-01-00647).

REFERENCES

1. M. Finkemeier and E. Mirkes, *Z. Phys. C* **72**, 619 (1996).
2. B. A. Li, *Phys. Rev. D* **55**, 1436 (1997).
3. S. Fajfer and J. Zupan, *Int. J. Mod. Phys. A* **14**, 4161 (1999).
4. A. A. Andrianov and V. A. Andrianov, *Int. J. Mod. Phys. A* **20**, 1850 (2005).
5. S. Nussinov and A. Soffer, *Phys. Rev. D* **80**, 033010 (2009).
6. N. Paver and Riazuddin, *Phys. Rev. D* **84**, 017302 (2011).
7. D. G. Dumm and P. Roig, *Phys. Rev. D* **86**, 076009 (2012).
8. R. Escribano, S. Gonzalez-Solis, and P. Roig, *J. High Energy Phys.* **1310**, 039 (2013).
9. R. Escribano, S. Gonzalez-Solis, M. Jamin, and P. Roig, *J. High Energy Phys.* **1409**, 042 (2014).
10. X.-W. Kang, B. Kubis, C. Hanhart, and U.-G. Meissner, *Phys. Rev. D* **89**, 053015 (2014).
11. T. Eguchi, *Phys. Rev. D* **14**, 2755 (1976).
12. D. Ebert and M. K. Volkov, *Z. Phys. C* **16**, 205 (1983).
13. M. K. Volkov, *Ann. Phys.* **157**, 282 (1984).
14. M. K. Volkov, *Sov. J. Part. Nucl.* **17**, 186 (1986).
15. D. Ebert and H. Reinhardt, *Nucl. Phys. B* **271**, 188 (1986).
16. U. Vogl and W. Weise, *Prog. Part. Nucl. Phys.* **27**, 195 (1991).
17. S. P. Klevansky, *Rev. Mod. Phys.* **64**, 649 (1992).
18. M. K. Volkov, *Phys. Part. Nucl.* **24**, 35 (1993).
19. D. Ebert, H. Reinhardt, and M. K. Volkov, *Prog. Part. Nucl. Phys.* **33**, 1 (1994).
20. M. K. Volkov and A. E. Radzhabov, *Phys. Usp.* **49**, 551 (2006).
21. M. K. Volkov and C. Weiss, *Phys. Rev. D* **56**, 221 (1997).
22. M. K. Volkov, *Phys. At. Nucl.* **60**, 1920 (1997).
23. M. K. Volkov, D. Ebert, and M. Nagy, *Int. J. Mod. Phys. A* **13**, 5443 (1998).
24. M. K. Volkov and V. L. Yudichev, *Phys. Part. Nucl.* **31**, 282 (2000).
25. A. I. Ahmadov and M. K. Volkov, *Phys. Part. Nucl. Lett.* **12**, 744 (2015).
26. M. K. Volkov and D. G. Kostunin, *Phys. Rev. D* **86**, 013005 (2012).
27. M. K. Volkov, A. B. Arbuzov, and D. G. Kostunin, *Phys. Rev. D* **86**, 057301 (2012).
28. M. K. Volkov, A. B. Arbuzov, and D. G. Kostunin, *Phys. Rev. C* **89**, 015202 (2014).
29. A. I. Ahmadov, Yu. L. Kalinovsky, and M. K. Volkov, *Int. J. Mod. Phys. A* **30**, 1550161 (2015).
30. M. K. Volkov and A. A. Pivovarov, *Mod. Phys. Lett. A* **31**, 1650043 (2016); arXiv:1511.08332 [hep-ph].
31. K. Inami et al. (Belle Collab.), *Phys. Lett. B* **672**, 209 (2009).
32. P. del Amo Sanchez et al. (BaBar Collab.), *Phys. Rev. D* **83**, 032002 (2011).
33. M. K. Volkov and V. L. Yudichev, *Eur. Phys. J. A* **10**, 109 (2001).
34. A. I. Ahmadov, D. G. Kostunin, and M. K. Volkov, *Phys. Rev. C* **87**, 045203 (2013).
35. K. A. Olive et al. (Particle Data Group), *Chin. Phys. C* **38**, 090001 (2014); update (2015).
36. D. Aston, N. Awaji, T. Bienz, et al., *Nucl. Phys. B* **296**, 493 (1988).
37. D. Aston, N. Awaji, J. D'Amore, et al., *Nucl. Phys. B* **292**, 693 (1987).